ISSN 2070-2051, Protection of Metals and Physical Chemistry of Surfaces, 2014, Vol. 50, No. 6, pp. 739–746. © Pleiades Publishing, Ltd., 2014.
Original Russian Text © S.N. Lanin, A.A. Bannykh, E.V. Vlasenko, N.V. Kovaleva, S.M. Levachev, R.F. Akhundov, 2014, published in Fizikokhimiya Poverkhnosti i Zashchita Materialov, 2014, Vol. 50, No. 6, pp. 608–615.

SEPARATION PROCESSES AT THE INTERFACES. CHROMATOGRAPHY

Adsorption Properties of Alumina Modified with Nickel Oxide Nanoparticles and Silver–Nickel Oxide Bimetallic Nanoparticles

S. N. Lanin, A. A. Bannykh, E. V. Vlasenko, N. V. Kovaleva, S. M. Levachev, and R. F. Akhundov

Department of Chemistry, Moscow State University, Moscow, Russia

e-mail: SNLanin@phys.chem.msu.ru

Received April 28, 2014

Abstract—The adsorption properties of γ-Al_2O_3, both in the original form and as modified with NiO nanoparticles and [NiO+Ag] bimetallic nanoparticles, were studied using the dynamic sorption method. n-Alkanes (C_6–C_8), benzene, chloroform, diethyl ether, toluene, and ethylbenzene were used as test adsorbates. The adsorption isotherms were measured, and the isosteric heats of adsorption of the tested adsobates were calculated. The surface of the original γ-Al_2O_3 was found to mostly have electron-accepting (acidic) properties, while the surface of alumina modified with NiO nanoparticles exhibits electron-donating (basic) properties. The adsorption isotherms of all adsorbates onto γ-Al_2O_3 at all specified temperatures lie higher than onto the original γ-Al_2O_3. Nanocomposite 5% NiO/γ-Al_2O_3 exhibits the highest adsorption activity with respect to aromatic hydrocarbons.

DOI: 10.1134/S2070205114060112

INTRODUCTION

NiO nanoparticles supported onto metal oxides exhibit the highest catalytic activity in a number of catalyzed reactions (in particular, in hydrodechlorination [1] and hydrogenation reactions, which include a large family of reactions of hydrogen attachment at unsaturated bonds in unsaturated and aromatic hydrocarbons [2], in selective oxidation of CO to CO_2 [3], and in toluene oxidation [4].

One of the main reasons for changes in the physical and chemical properties of nanoparticles is an increase in the fraction of surface atoms exposed to conditions (the coordination number, local symmetry, etc.) different from those for the atoms inside a bulky phase. The fraction of surface atoms decreases with increasing particle size [5].

The adsorption and catalytic properties of metal nanoparticles and their oxides depend on the nature of precursor solution, on the type of its interactions with the support, on chemical nature of the support, on preparation conditions, and size of resulting particles [6].

Adsorption of molecules of the original compounds, chemical conversion of the adsorbed compounds, and subsequent desorption of the reaction products occur on the catalyst surface during a catalytic reaction. In order to understand the mechanism of catalytic reactions occurring on immobilized nanoparticles of metals and their oxides, the data on the force and nature of their interaction with supports and reagents needs to be available [7–10].

This work was aimed at studying the adsorption properties of γ-Al_2O_3, both the original one (which is widely used as a support in heterogeneous catalysts for various processes) and the one modified with NiO nanoparticles and [NiO + Ag] bimetallic nanoparticles via dynamic adsorption at low surface coverage.

EXPERIMENTAL

Adsorbents. We used original γ-Al_2O_3 (Sigma-Aldrich; specific surface area of 110 m^2/g, average pore volume of 0.29 cm^3/g, pore diameter of 340 Å), and γ-Al_2O_3-based nanocomposites ([0.5%NiO + 0.5%Ag]/γ-Al_2O_3 and [2.5%NiO + 2.5%Ag]/γ-Al_2O_3) were used as adsorbents.

Synthesis of nanocomposites. γ-Al_2O_3 and NaOH were sequentially added to the aqueous solution of nickel(II) chloride preheated to 50–90°C. After the mixture was cooled, sodium tetrahydroborate solution in an aliphatic alcohol was added. The azeotropic mixture of aliphatic alcohol and water was distilled off the resulting product; the product was kept at 70–90°C for 30 min and washed once with water and twice with ethanol; the precipitate was kept in air at 50°C for 2 h until nickel was completely oxidized to nickel(II) oxide. The equations of the reactions occurring during synthesis of nickel oxide nanoparticles can be written as follows:

$$NiCl_2 \cdot 6H_2O + 2NaBH_4 \rightarrow Ni + 2B(OH)_3 + 2NaCl + 7H_2\uparrow,$$

$$Ni + \frac{1}{2}O_2 \rightarrow NiO.$$

A solution containing preset amounts of silver nitrate and nickel(II) chloride was used instead of the

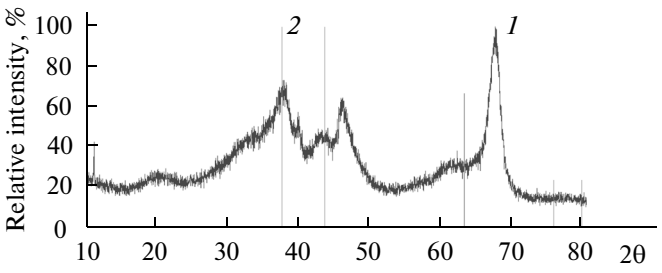

Fig. 1. X-ray diffraction pattern of the 10% NiO/γ-Al_2O_3 composite (*1*) with the superimposed X-ray diffraction pattern of the NiO phase (*2*).

aqueous solution of nickel(II) chloride to fabricate bimetallic [NiO + Ag]/γ-Al_2O_3 nanocomposites [11].

Nanocomposite samples were studied by X-ray diffraction on a Rigaku D/MAX 2500 diffractometer with a rotating anode (Japan).

We used the XRD patterns (Fig. 1) and the Debye–Scherrer equation [12] (Eq. (1)) to estimate the average diameter (D_{hkl}) of NiO nanoparticles.

$$D_{hkl} = \frac{k\lambda}{\beta_{hkl}\cos\theta_{hkl}}, \quad (1)$$

where k is the dimensionless form factor ($k = 0.89$); λ is the irradiation wavelength, Å; θ_{hkl} is the diffraction angle; and β_{hkl} is the half-width of the diffraction peak (radians).

Table 1 lists the results of calculation of particle size.

Adsorbates. We used n-alkanes (C_6–C_8), benzene, toluene, ethylbenzene, chloroform, and diethyl ether as adsorbates to study the texture and chemistry of μ-Al_2O_3 surface, both original and modified with nanoparticles. Parameters of these compounds are given in Table 2.

Adsorption studies. Adsorption properties were studied by dynamic vapor sorption on a Crystal Lux 4000M chromatograph with a thermal conductivity detector. To perform physicochemical measurements, we used 20-cm-long glass columns with an internal diameter of 2 mm. Helium was used as a carrier gas; its flow rate was 30 mL/min. Prior to measurements, the sample was kept in the chromatograph chamber in a flow of the carrier gas at 200°C for 3 h. The volume of adsorbate sample injected with a microsyringe was varied from 0.5 to 10 μL.

Table 1. Average size of NiO nanoparticles, nm

Composite	Nanoparticle size, nm
5% NiO/γ-Al_2O_3	3.7
10% NiO/γ-Al_2O_3	7.1
[0.5% Ag + 0.5% NiO]/γ-Al_2O_3	4.7
[2.5% Ag + 2.5% NiO]/γ-Al_2O_3	7.4

At low degrees of surface coverage, we measured the specific retention volumes, determined the adsorption isotherms, and calculated the isosteric heats of adsorption via procedure [13] for n-C_6H_{14}, C_6H_6, $CHCl_3$, and $(C_2H_5)_2O$ at 100, 110, and 120°C; for $C_6H_5CH_3$ at 130, 140, and 150°C; and for $C_6H_5C_2H_5$ at 150, 160, and 170°C.

RESULTS AND DISCUSSION

Adsorption isotherms of n-hexane, benzene, toluene, and ethylbenzene on the original γ-Al_2O_3 and that modified with nickel oxide nanoparticles are shown in Fig. 2. All the isotherms are convex facing the adsorption axis, attesting to the fact that the adsorbate–adsorbent interaction is stronger than the adsorbate–adsorbate one. At identical equilibrium pressures, adsorption of all the adsorbates onto the original and modified γ-Al_2O_3 samples decreases with increasing temperature (Fig. 2), being indicative of the physical nature of the adsorption.

Figure 3 shows the sorption isotherms of benzene at 100°C onto bimetallic [NiO + Ag]/γ-Al_2O_3 nanocomposites and NiO/γ-Al_2O_3 nanocomposites. Adsorption of all the adsorbates at identical equilibrium pressures decreased for the following series: 5% NiO/γ-Al_2O_3 > 10% NiO/γ-Al_2O_3 > [2.5% NiO + 2.5% Ag]/γ-Al_2O_3 > γ-Al_2O_3 > [0.5% NiO + 0.5% Ag]/γ-Al_2O_3, which correlates with the average size of immobilized mono- and bimetallic nanoparticles (Table 1).

Figure 4 shows the adsorption isotherms of toluene and ethylbenzene at different temperatures onto the original γ-Al_2O_3 and 5%NiO/γ-Al_2O_3 nanocomposite. One can see how the adsorption values decrease stepwise with increasing temperature; at each point, the adsorption isotherms of toluene and ethylbenzene onto 5%NiO/γ-Al_2O_3 composite lie noticeably higher than those for the original γ-Al_2O_3.

The specific surface areas (s, m^2/g) and monolayer capacities a_m for the samples under study were calculated using the adsorption isotherms of hexane at 100°C and the BET method. Parameters of microporous structure were estimated using the adsorption isotherms of benzene and the Dubinin–Radushkevich equation [14]. The micropore radius (R) was calculated based on the dependence of characteristic adsorption energy (E_0) using the equation $R = 12/E_0$ [15]. The calculated data are listed in Table 3. It is clear from Table 3 that immobilization of both mono- and bimetallic nanoparticles onto the γ-Al_2O_3 surface reduces the specific surface area of the nanocomposites by 20–30% compared to the original support (γ-Al_2O_3), while the characteristic adsorption energy increases by ~0.5–3 kJ/mol. The micropore radius decreases for all nanocomposites.

Table 2. Characteristics of the adsorbates tested (*M* is the molecular weight; μ is the dipole moment; α is the total polarizability of a molecule; and AN and DN are the electron-accepting and electron-donating energy parameters of molecules, respectively [6])

Adsorbate	*M*	μ, D	α, Å^3	*DN*, kJ/mol	*AN*
n-C_6H_{14}	86.2	0	11.9	0	0
n-C_7H_{16}	100.2	0	13.7	0	0
C_6H_6	78.1	0	10.4	0.4	8.2
$C_6H_5CH_3$	92.1	0.37	12.2	–	–
$C_6H_5C_2H_5$	106.2	0.59	14.1	–	–
$CHCl_3$	119.4	1.15	8.2	0	23.0
$(C_2H_5)_2O$	79.1	1.70	9.0	80.3	3.9

Heats of Adsorption

By definition, the surface of the synthesized nanocomposites is heterogeneous both in terms of their chemistry and energy. The reason is that the greatest part of the γ-Al_2O_3 surface is covered with nickel oxide nanoparticles that block the most active sites of the original γ-Al_2O_3 on one hand and act as active adsorption sites on the other hand. Thus, active sites of immobilized nickel oxide and silver nanoparticles make the decisive contribution to the changes in adsorption activity of the synthesized nanocomposites. It is clear that several types of active sites, formed both by the original γ-Al_2O_3 structure and by the supported nanoparticles, will sequentially participate in the adsorption. In order to test this assumption, we used the empirical Freundlich equation describing adsorption onto heterogeneous surfaces,

$$a = kp^n, \tag{2}$$

and the Langmuir equation (the equation of localized adsorption onto homogeneous surface in the absence of any strong interactions between adsorbate molecules),

$$a = \frac{a_m Kp}{1 + Kp}, \tag{3}$$

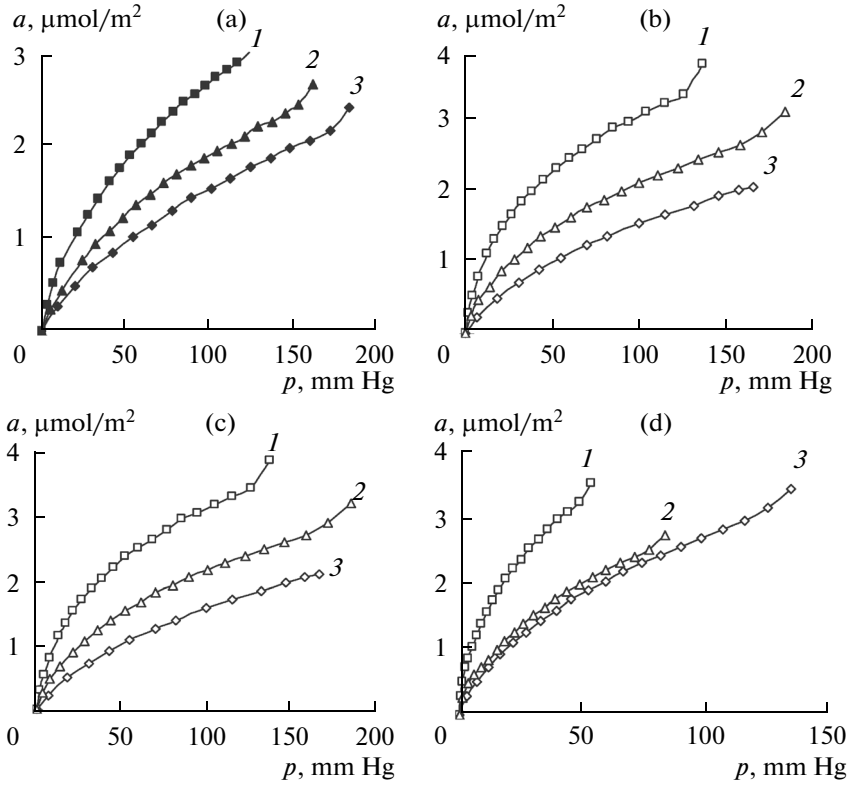

Fig. 2. Adsorption isotherms of (*a*) *n*-C_6H_{14} at 100°C, (b) C_6H_6 at 100°C, (c) $C_6H_5CH_3$ at 150°C, and (d) $C_6H_5C_2H_5$ at 150°C onto composites: (*1*) 5%NiO/γ-Al_2O_3, (*2*) 10%NiO/γ-Al_2O_3, and (*3*) γ-Al_2O_3.

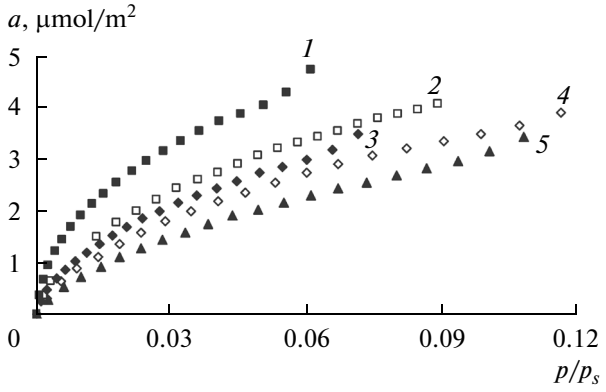

Fig. 3. Adsorption isotherms of C_6H_6 at 100°C onto (*1*) 5%NiO/γ-Al_2O_3, (*2*) 10%NiO/γ-Al_2O_3, (*3*) [2.5%NiO + 2.5%Ag]/γ-Al_2O_3, (*4*) the original γ-Al_2O_3, and (*5*) [0.5%NiO + 0.5% Ag]/γ-Al_2O_3 nanocomposites.

where a is the adsorption, a_m is monolayer capacity, K is the equilibrium constant, and p is the adsorbate pressure in the gas phase.

Figure 5 shows the adsorption isotherms of benzene onto 5%NiO/γ-Al_2O_3 nanocomposite in the linear coordinates of the Freundlich equation. It is clear that the isotherms are almost ideally linear when presented in logarithmic coordinates.

The adsorption isotherms in the linear form of the Langmuir equation are shown in Fig. 6. Three linear regions were distinguished on each isotherm, indicating that there are three homogeneous surface areas that differ in their adsorption properties and constitute the homogeneous surface together: the regions corresponding to low concentrations (I), medium concentrations (II), and relatively high concentrations (III). The monolayer capacities a_m, equilibrium constants K, Henry constants K_H and $K_{H,calc} = a_mK$ were determined for these homogeneous surface areas. The K values of all sorbates decrease with increasing temperature both for the intact and modified alumina.

At low degrees of surface coverage (region I in Fig. 5), the K_p values are much lower than unity (Table 4); hence, the K_p value in the denominator can be neglected and in this case

$$a = a_mKp. \quad (4)$$

Thus, the adsorption value is proportional to adsorbate pressure in the gas phase, and the Langmuir equation is converted to the Henry equation.

$$a = K_pp. \quad (5)$$

We used the inverse temperature dependence of $\ln K_H$ to calculate heats of adsorption Q in the Henry's region (region I); their values are listed in Table 5. The heats of adsorption of the tested compounds onto 5% NiO/Al_2O_3 are considerably higher, while the heats of adsorption onto 10% NiO/Al_2O_3 are also higher for n-hexane and ethylbenzene and slightly lower for benzene and toluene than those of adsorption onto γ-Al_2O_3.

We used the adsorption isotherms to calculate the isosteric heats of adsorption (Q_{st}) at low degrees of surface coverage ($a = 0.35$ μmol/m²) for all the nanocomposites studied (Table 6). It can be seen from Table 6 that low heats of adsorption of $CHCl_3$ (its molecules exhibiting electron-accepting properties; $DN = 0$, $AN = 23$) and high heats of adsorption for $(C_2H_5)_2O$ molecules (with electron-donating properties predominating; DN = 80, AN = 3.9) onto the original γ-Al_2O_3 indicate that the surface of the original γ-Al_2O_3 exhibits electron-accepting (acidic) properties. In turn, the lower heats of adsorption of $(C_2H_5)_2O$ compared to those of $CHCl_3$ onto NiO/γ-Al_2O_3 composites attest to the predominantly electron-donating (basic) properties of their surface. An increase in heats of adsorption onto NiO/γ-Al_2O_3 was also observed for benzene molecules (with electron-accepting properties predominating; $DN = 0.4$, $AN = 8.2$).

The heats of adsorption of n-C_6H_{14} (molecules of which can be adsorbed only due to nonspecific dispersion interactions) onto NiO/γ-Al_2O_3 increased abruptly compared to the original γ-Al_2O_3. Immobili-

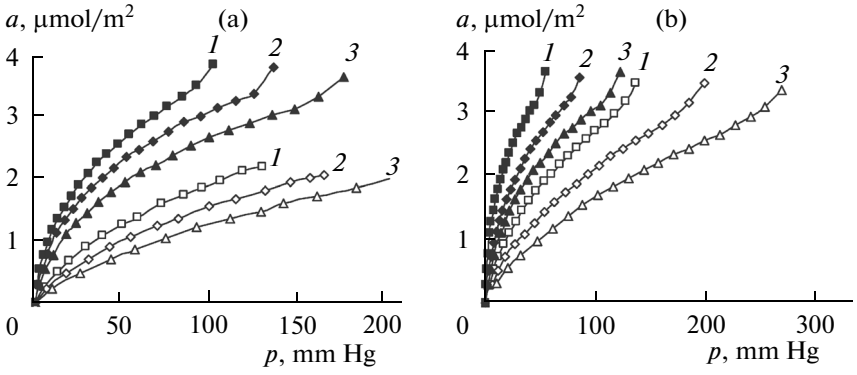

Fig. 4. Adsorption isotherms of (a) $C_6H_5CH_3$ and (b) $C_6H_5C_2H_5$ onto γ-Al_2O_3 (white markers) and onto 5% NiO/γ-Al_2O_3 nanocomposite (black markers): (a): (*1*) 140, (*2*) 150, and (*3*) 160°C; (b): (*1*) 150, (*2*) 160, and (*3*) 170°C.

Table 3. Parameters of the microporous structure of γ-Al_2O_3 and composites

Adsorbent	S, m^2/g	a_m, μmol/g	E_0, kJ/mol	R, nm
γ-Al_2O_3	98	275	10.3	1.16
5% NiO/γ-Al_2O_3	57	181	13.2	0.91
10% NiO/γ-Al_2O_3	70	222	12.1	0.99
[0.5% NiO + 0.5% Ag]/γ-Al_2O_3	74	237	12.2	0.99
[2.5% NiO + 2.5% Ag]/γ-Al_2O_3	73	232	10.8	0.91

Table 4. Products K_p calculated at the initial regions of the adsorption isotherms

Adsorbate	C_6H_{14}	C_6H_6	$C_6H_5CH_3$	$C_6H_5C_2H_5$
γ-Al_2O_3	0.11	0.17	0.16	0.16
5% NiO/γ-Al_2O_3	0.17	0.22	0.16	0.32
10% NiO/γ-Al_2O_3	0.10	0.11	0.39	0.14

zation of nanoparticles reduced the effective pore diameter of the support (Table 3), as a certain number of pores were blocked by nanoparticles. The adsorption potential of nanocomposites increases, resulting in a consistent rise in the heats of adsorption.

The contribution of energy of specific interactions (Q_{spec}) to the total energy of adsorption onto NiO/γ-Al_2O_3 and [Ag + NiO]/γ-Al_2O_3 composites as compared to the original γ-Al_2O_3 decreased both for the electron-accepting ($CHCl_3$) and for electron-donating ($(C_2H_5)_2O$) molecules.

The heats of adsorption of aromatic hydrocarbons (benzene, toluene, and ethylbenzene), the molecules of which comprise a conjugated π-system, onto the original γ-Al_2O_3 and modified samples are higher than those of n-hexane (Table 6) due to formation of π-complexes of these molecules with active sites residing on the sorbent surface. The increase in basic properties of the molecules after alkyl moieties are added to the aromatic ring causes stronger adsorption of toluene and ethylbenzene, in particular, compared with nonsubstituted benzene.

The initial heats of adsorption of ethylbenzene are significantly higher than the heats of adsorption of benzene onto γ-Al_2O_3 due to the strong interaction between the π-electrons of the aromatic ring of ethylbenzene (which is additionally enriched in electron density due to the ethyl moiety) with electron-accepting sites on the surface. For NiO/γ-Al_2O_3 and [NiO + Ag]/γ-Al_2O_3 composites, there is also interaction with active sites of NiO and [NiO + Ag] nanoparticles, respectively. At adsorption a = 0.35 μmol/m^2, the heats of adsorption of ethylbenzene are higher than the heats of adsorption of benzene onto NiO/γ-Al_2O_3

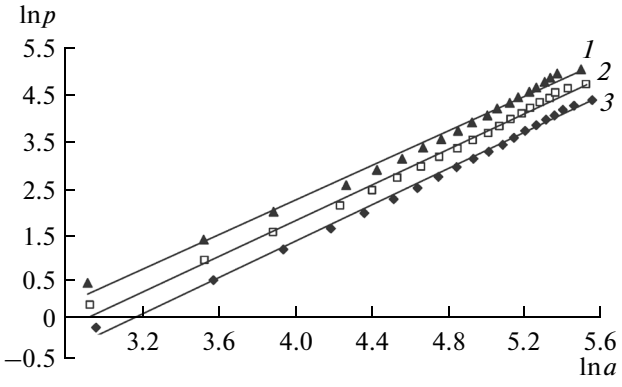

Fig. 5. Adsorption isotherms of C_6H_6 onto 5% NiO/γ-Al_2O_3 nanocomposite in linear coordinates of the Freundlich equation: (*1*) 120, (*2*) 110, and (*3*) 100°C.

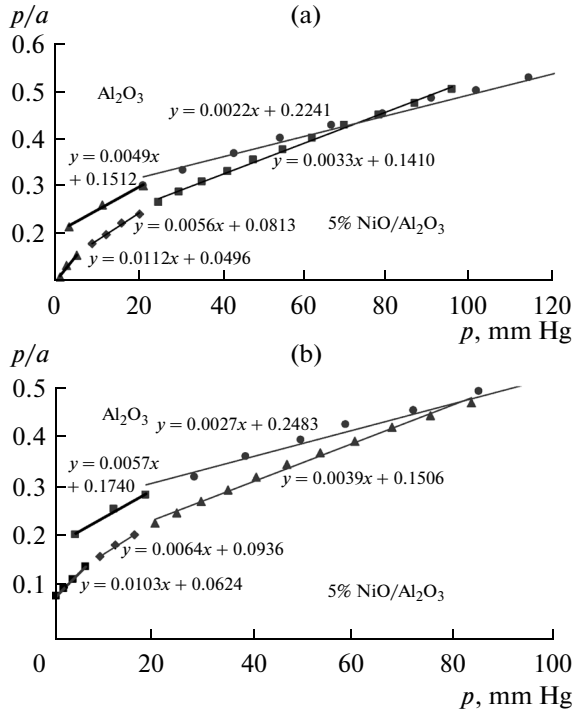

Fig. 6. Adsorption isotherms of (a) C_6H_6 at 110°C and (b) $C_6H_5CH_3$ at 140°C onto γ-Al_2O_3 and 5% NiO/γ-Al_2O_3 nanocomposite in linear Langmuir coordinates.

Table 5. Heats of adsorption, Q_{st}, kJ/mol, of the tested compounds adsorbed in the Henry region onto the original γ-Al_2O_3 and 5% NiO/γ-Al_2O_3 and 10% NiO/γ-Al_2O_3 nanocomposites

Adsorbate	Al_2O_3	5% NiO/Al_2O_3	10% NiO/Al_2O_3
n-C_6H_{14}	40	51	46
C_6H_6	55	59	53
$C_6H_5CH_3$	63	75	60
$C_6H_5C_2H_5$	86	105	104

Table 6. Isosteric heats of adsorption (Q_{st}, kJ/mol) of the tested adsorbates onto the original γ-Al_2O_3 and 5% NiO/γ-Al_2O_3, 10% NiO-γ-Al_2O_3, [0.5Ag + 0.5% NiO]/γ-Al_2O_3, and [2.5% Ag + 2.5% NiO]/γ-Al_2O_3 nanocomposites at the degree of surface coverage $a = 0.35$ μmol/m^2

Adsorbate	Q_{st}	Q_{disp}	Q_{spec}	Q_{st}	Q_{disp}	Q_{spec}	Q_{st}	Q_{disp}	Q_{spec}	Q_{st}	Q_{disp}	Q_{spec}	Q_{st}	Q_{disp}	Q_{spec}
	γ-Al_2O_3			5% NiO/γ-Al_2O_3			10% NiO/γ-Al_2O_3			[0.5% Ag + 0.5% NiO]/γ-Al_2O_3			[2.5% Ag + 2.5% NiO]/γ-Al_2O_3		
n-C_6H_{14}	35			48			45			47			45		
n-C_7H_{16}	53			54			53			51			50		
n-C_8H_{18}	67			60			61			54			55		
C_6H_6	54	28	26	58	43	15	59	39	20	51	46	6	53	41	12
$CHCH_3$	58	11	47	63	36	27	61	29	32	54	42	12	59	35	24
$(C_2H_5)_2O$	83	21	62	59	40	19	52	35	17	62	44	18	60	39	21
$C_6H_5CH_3$	62	41	21	71	49	22	67	46	21	55	49	6	64	46	18
$C_6H_5C_2H_5$	74	56	18	93	55	38	83	55	28	73	52	21	78	51	27

composite by 35 kJ/mol; onto 10% NiO/γ-Al_2O_3, by 24 kJ/mol; onto [0.5% NiO + 0.5% Ag]/γ-Al_2O_3, by 22 kJ/mol; and onto [2.5% NiO + 2.5% Ag]/γ-Al_2O_3, by 25 kJ/mol.

The heats of adsorption of toluene are higher than those of benzene by only 5–10 kJ/mol on average. This is typical both of the original γ-Al_2O_3 and of all the nanocomposites studied and is presumably caused by the fact that toluene and benzene have similar structures, as opposed to ethylbenzene.

The energy of specific interactions is determined by electron-donating and electron-accepting properties of adsorbate molecules and the adsorbent surface and can be written as the following expression [10]:

$$Q_{spec.}/AN = K_D + K_A DN/AN, \quad (6)$$

where K_A and K_D are the electron-accepting and electron-donating energy parameters of the surface and *AN* and *DN* are the electron-accepting and electron-donating parameters of adsorbate molecules.

Table 7 lists the electron-accepting (K_A) and electron-donating (K_D) energy parameters of the surface of the original γ-Al_2O_3 and NiO/γ-Al_2O_3 nanocomposites determined using this equation.

The dependences of the isosteric heats of adsorption Q_{st} on the degree of surface coverage were determined from adsorption isotherms calculated using the empirical Freundlich equation for a heterogeneous surface in its logarithmic form (with coefficient $R^2 = 0.999$).

$$\ln a = \ln K + n \ln p. \quad (7)$$

The calculated isosteric heats are shown in Tables 8 and 9.

Tables 8 and 9 show that the Q_{st} for aromatic hydrocarbons adsorbed onto NiO/γ-Al_2O_3 composites are higher than those for [NiO + Ag]/γ-Al_2O_3 composites for all degrees of surface coverage, which indicates that NiO/γ-Al_2O_3 composites have a higher adsorption activity than that of [NiO + Ag]/γ-Al_2O_3.

The heats of adsorption of all adsorbates decrease with increasing average size of immobilized nanoparticles. Higher heats of adsorption are typical of the most active surface areas that are the first to be covered with adsorbate molecules. After they are covered, adsorption takes place at sites with lower activity, and the heats of adsorption decrease gradually. NiO nanoparticles are the most active sites on the surface of NiO/γ-Al_2O_3 composites. The surface of the original γ-Al_2O_3 under conditions under study can contain only hydroxyl moieties, since it was heated to temperatures higher than 200°C either at the preparation and nanoparticle supporting stage nor during the adsorption experiments. Dehydroxylation of the Al_2O_3 surface starts at temperatures higher than 200°C [16].

An analysis of the experimental data indicates that the heats of adsorption are determined by the composition and structure of the composite surface. In terms of heats of adsorption of aromatic hydrocarbons, the composites can be arranged into the following series: NiO/γ-Al_2O_3 > 10% NiO/γ-Al_2O_3 > [2.5% NiO + 2.5% Ag]/γ-Al_2O_3 > [0.5% NiO + 0.5% Ag]/γ-Al_2O_3.

Table 7. Electron-accepting (K_A) and electron-donating (K_D) energy parameters of the surface of the original γ-Al_2O_3 and nanocomposites based on it

Adsorbent	K_A	K_D, kJ/mol	K_A/K_D	$(K_D^0 - K_D)/K_D^0$	$(K_A^0 - K_A)/K_A^0$
Al_2O_3	0.67	2.02	0.33	1.00	1.00
5% NiO/Al_2O_3	0.18	1.16	0.16	0.43	0.73
10% NiO/Al_2O_3	0.15	1.38	0.11	0.32	0.78
[0.5% NiO + 0.5% Ag]/Al_2O_3	0.20	0.52	0.38	0.74	0.70
[2.5% NiO + 2.5% Ag]/Al_2O_3	0.22	1.03	0.21	0.49	0.67

K_D^0 is the electron-donating number of the original γ-Al_2O_3.

K_A^0 is the electron-accepting number of the original γ-Al_2O_3.

Table 8. Isosteric heats (Q_{st}, kJ/mol) of the tested adsorbates as functions of the degree of coverage up to the monolayer

a/s, μmol/m^2	C_6H_{14}	C_6H_6	$C_6H_5CH_3$	$C_6H_5C_2H_5$
γ-Al_2O_3				
0.35	34.8	54.3	61.8	84.0
0.4	34.4	53.8	60.5	83.3
0.5	33.8	52.8	58.4	79.5
0.6	33.2	52.0	56.9	77.1
0.7	33.0	51.6	56.8	76.2
0.8	32.6	51.0	54.5	74.5
0.9	32.4	50.6	53.3	73.4
1.0	32.1	50.2	52.8	72.8
5% NiO/γ-Al_2O_3				
0.35	48.6	58.2	71.0	92.5
0.45	47.5	56.8	69.1	89.3
0.55	46.4	55.8	67.5	86.8
0.65	45.7	55.1	66.4	84.9
0.8	44.9	54.3	64.8	82.9
0.9	43.9	53.3	63.6	80.3
1.0	43.3	52.8	62.9	79.1
10% NiO/γ-Al_2O_3				
0.35	45.2	58.6	66.6	82.9
0.5	43.8	55.7	63.4	76.7
0.6	43.1	54.5	62.1	74.1
0.7	42.3	52.8	60.2	70.6
0.8	41.9	51.9	59.3	68.8
0.9	41.5	51.1	58.4	67.1
1.0	40.6	49.8	57.0	64.1

Table 9. Isosteric heats (Q_{st}, kJ/mol) of the tested adsorbates as functions of the degree of coverage up to the monolayer

a/s, μmol/m^2	C_6H_{14}	C_6H_6	$C_6H_5CH_3$	$C_6H_5C_2H_5$	C_6H_{14}	C_6H_6	$C_6H_5CH_3$	$C_6H_5C_2H_5$
[0.5% NiO + 0.5% Ag]/γ-Al_2O_3					[2.5% NiO + 2.5% Ag]/γ-Al_2O_3			
0.35	47.4	51.0	55.3	72.7	45.1	52.8	57.9	66.6
0.45	46.2	49.9	54.1	71.0	44.3	52.1	56.1	65.1
0.55	45.3	49.1	53.2	69.7	43.7	51.5	54.7	63.9
0.6	44.8	48.6	52.8	69.0	43.3	51.2	53.9	63.3
0.7	44.1	48.0	52.1	68.0	42.9	50.7	52.8	62.4
0.8	43.5	47.5	51.5	67.2	42.5	50.4	52.1	61.7
0.9	42.9	47.0	51.0	66.3	42.1	49.9	51.0	60.8
1.0	42.4	46.5	50.5	65.6	41.7	49.6	50.3	60.2

Bimetallic [NiO + Ag]/γ-Al_2O_3 composites exhibit lower adsorption activity.

The adsorption and catalytic activity of [Au–Ni + Ag]/γ-Al_2O_3 nanocomposite fabricated by metal-vapor synthesis increased abruptly compared to the sample containing gold only [17]. The authors attributed it to the fact that nickel interacts with gold to form the mixed Au–Ni particles under the synthesis conditions. Electron-deficient nickel pulls electron density away from Au^0, thus forming the active catalytic site Au^{+1}.

The mixed structures of Ni–Ag nanoparticles (formed according the shell–nucleus principle) with Ag residing in the shell and Ni residing in the nucleus exhibit high catalytic properties, resulting in a shift in electron density from Ag^0 to the electron-deficient d-orbital of nickel [18].

It is possible that a somewhat different structure of bimetallic particles (having weaker donating–accepting metal–metal interactions) could be formed in our case during modification of γ-Al_2O_3 with [Ni + Ag] nanoparticles followed by oxidation of Ni nanoparticles to NiO.

Hence, we demonstrated that the thermodynamic parameters of adsorption are dependent on the degree of surface coverage, the average size of mono- and bimetallic particles, as well as on the amount of metal coated onto the support surface. The surface sites of 5% NiO/γ-Al_2O_3 and 10% NiO/γ-Al_2O_3 nanocomposites exhibit the strongest adsorption properties with respect to aromatic compounds.

ACKNOWLEDGMENTS

This work was supported by the Russian Foundation for Basic Research, project no. 12-03-00595.

REFERENCES

1. Kachinskii, S.A., Golubina, E.V., Lokteva, E.S., and Lunin, V.V., *Russ. J. Phys. Chem. A*, 2007, vol. 81, no. 6, p. 886.
2. Navalikhina, M.D. and Krylov, O.V., *Usp. Khim.*, 1998, vol. 67, p. 656.
3. Levent, M., Gunn, D.J., and El-Bousiffi, M.A., *Hydrogen Energy*, 2003, vol. 28, p. 945.
4. Kim, K.-D., Nam, J.W., Seo, O.S., et al., *J. Phys. Chem. C*, 2011, vol. 115, p. 22954.
5. Bukhtiyarov, V.I. and Slin'ko, M.G., *Usp. Khim.*, 2001, vol. 70, p. 167.
6. Pichugina, D.A., Lanin, S.N., Kovaleva, N.V., et al., *Russ. Chem. Bull.*, 2010, vol. 59, p. 2039.
7. Lanin, S.N., Pichugina, D.A., Shestakov, A.F., et al., *Russ. J. Phys. Chem. A*, 2010, vol. 84, no. 12, p. 2133.
8. Lanin, S.N., Vinogradov, A.E., Vlasenko, E.V., et al., *Prot. Met. Phys. Chem. Surf.*, 2011, vol. 47, no. 6, p. 738.
9. Pichugina, D.A., Lanin, S.N., Beletskaya, A.V., et al., *Russ. J. Phys. Chem. A*, 2012, vol. 86, no. 12, p. 1892.
10. Lanin, S.N., Bannykh, A.A., and Kovaleva, N.V., *Russ. J. Phys. Chem. A*, 2013, vol. 87, no. 11, p. 1881.
11. Levachev, S.M., Levacheva, I.S., Lanin, S.N., et al., RF Patent 2496576.
12. Patterson, A.L., *Phys. Rev.*, 1939, vol. 56, p. 978.
13. *Eksperimental'nye metody v adsorbtsii i khromatografii* (Experimental Methods in Adsorption and Chromatography) Nikitin, Yu.S., Petrova, R.S., Eds., Moscow: Moscow Gos. Univ., 1990.
14. Dubinin, M.M., *Adsorbtsiya i poristost'* (Adsorption and Porosity),1972.
15. Plavnik, G.M. and Dubinin, M.M., *Izv. Akad. Nauk SSSR, Ser. Khim.*, 1966, p. 628.
16. Kiselev, A.V. and Lygin, V.I., *Infrakrasnye spektry poverkhnostnykh soedinenii i adsorbirovanakh veshchestv* (Infrared Spectra of Surface Compounds and Adsorbed Substances), Moscow: Nauka, 1972.
17. Nikolaev, S.A., *Cand. Sci. (Chem.) Dissertation*, Moscow: Moscow State Univ., 2006.
18. Ferrando, R., Jellinek, J., and Johnston, R.L., *Chem. Rev.*, 2008, vol. 108, p. 845.

Translated by D. Terpilovskaya